

# Vacancy diffusion in the Cu(001) surface I: an STM study

R. van Gastel <sup>a,\*</sup>, E. Somfai <sup>b,1</sup>, S.B. van Albada <sup>a</sup>, W. van Saarloos <sup>b</sup>,  
J.W.M. Frenken <sup>a</sup>

<sup>a</sup> *Kamerlingh Onnes Laboratory, Universiteit Leiden, P.O. Box 9504, 2300 RA Leiden, The Netherlands*

<sup>b</sup> *Instituut-Lorentz, Universiteit Leiden, P.O. Box 9506, 2300 RA Leiden, The Netherlands*

Received 11 January 2001; accepted for publication 16 August 2002

---

## Abstract

We have used the indium/copper surface alloy to study the dynamics of surface vacancies on the Cu(001) surface. Individual indium atoms that are embedded within the first layer of the crystal, are used as probes to detect the rapid diffusion of surface vacancies. STM measurements show that these indium atoms make multi-lattice-spacing jumps separated by long time intervals. Temperature dependent waiting time distributions show that the creation and diffusion of thermal vacancies form an Arrhenius type process with individual long jumps being caused by one vacancy only. The length of the long jumps is shown to depend on the specific location of the indium atom and is directly related to the lifetime of vacancies at these sites on the surface. This observation is used to expose the role of step edges as emitting and absorbing boundaries for vacancies.

© 2002 Elsevier Science B.V. All rights reserved.

*Keywords:* Scanning tunneling microscopy; Surface diffusion; Copper; Indium; Surface defects

---

## 1. Introduction

Over the past decade the scanning tunneling microscope (STM) [1] has been the predominant instrument that has been employed to study atomic-scale diffusion processes on surfaces. Many STM studies of surface diffusion phenomena have now been performed investigating the mobility of steps [2–5], islands [6,7] and adsorbates [8]. The

STM has also been the instrument of choice in the study of adatom diffusion and the role of adatom diffusion processes in crystal growth [9]. However, the study of the diffusion of *naturally* occurring adatoms and vacancies is hampered by the finite temporal resolution of the STM. Adatoms and vacancies both involve two energy parameters, a formation energy and a diffusion barrier. Typically, the values of these parameters are such that either species is present only in very low numbers, while being extremely mobile, far too mobile to be imaged with an STM. Lowering the temperature to reduce the diffusion rate, so that it can be monitored with an STM, also causes the density of naturally occurring adatoms and vacancies to drop to extremely low values, so low that no vacancies and adatoms can anymore be observed. The study

---

\* Corresponding author. Present address: Surface and Interface Sciences Department, Sandia National Laboratories, P.O. Box 5800, Mail Stop 1415, Albuquerque, NM 87185-1415, USA.

<sup>1</sup> Present address: Department of Physics, University of Warwick, Coventry, CV4 7AL, UK.

of adatom diffusion with field ion microscopy (FIM) or STM [9,10] has been made possible though by the simple fact that adatoms can be deposited on a surface at low temperatures from an external evaporation source. In the case of FIM, they can also be produced by means of field evaporation [11,12]. No such possibility exists for surface vacancies and it is for this reason that the role of monatomic surface vacancies in the atomic-scale dynamics of single crystal metal surfaces has remained relatively unexposed so far.

In this paper we present a detailed study of the diffusion of monatomic vacancies in the first layer of Cu(001). For this purpose we employ indium atoms that are embedded in the outermost copper layer. We show that the indium atoms diffuse through the first layer with the assistance of surface vacancies [13,14]. The details of the motion of the indium contain information on the diffusion of the surface vacancies. The theoretical framework which we use to interpret our measurements is described in full in the accompanying paper, which we shall refer to as paper II [15]. The diffusion of vacancies leads to an unusual, concerted type of motion of surface atoms and causes significant mobility of the Cu(001) surface as a whole at temperatures as low as room temperature.

## 2. Experimental procedures

The Cu sample ( $4.8 \times 4.8 \times 2.0 \text{ mm}^3$ ) was spark cut from a 5N-purity single crystal ingot. The crystal was chemically etched and then polished parallel to the (001)-plane [16]. Prior to mounting the crystal in the UHV system, we heated it to 1150 K for 24 h in an Ar/H<sub>2</sub> (20:1) atmosphere to remove sulphur impurities from the bulk of the crystal. After introduction into the vacuum chamber, the sample surface was further cleaned through several tens of cycles of sputtering with 600 eV Ar<sup>+</sup> ions and annealing to 675 K. Initially, after approximately every fifth cycle the surface was exposed to a few Langmuir of O<sub>2</sub> at a temperature of 550 K to remove carbon contamination from the surface. The frequency with which the surface was exposed to oxygen was lowered as the preparation progressed.

All experiments were performed with the programmable temperature STM constructed by Hoogeman et al. [17]. At the start of the experiments, STM images showed a clean, well-ordered surface with terrace widths up to 8000 Å. Small quantities of indium were deposited on the surface from a Knudsen cell.

## 3. Vacancy-mediated surface diffusion

Vacancies have been invoked in the past to explain the incorporation of foreign atoms into a surface [18–20] or the ripening of adatom islands [21]. The vacancy-mediated diffusion mechanism of embedded atoms was first proposed for the motion of Mn atoms in Cu(001) during the formation of a surface alloy [22,23]. Our STM investigation of the diffusion of indium atoms embedded within the first layer of a Cu(001) surface was the first to prove unambiguously that this motion takes place with the help of surface vacancies [13,14]. More recently, Pd atoms were shown to diffuse through the Cu(001) surface by the same diffusion mechanism [24]. In this section, we show how we can conclude that the indium atoms diffuse through the surface with the help of surface vacancies, without being able to observe them directly.

The starting point of our observations is shown in Fig. 1. At 38 min after the deposition of 0.03 ML of indium at room temperature, the image shows a high density of indium atoms in the area around a step edge. STM images measured with bias voltages ranging from  $-0.10$  to  $-2.18$  V always showed the indium atoms as bright protrusions with an approximate height of 0.4 Å. Comparison of the apparent height of the indium atoms observed in this image with that of indium adatoms that were observed on the Cu(1117) surface ( $\approx 2.55$  Å) [25], shows that the indium atoms in Fig. 1 are indeed embedded in the first layer of the crystal. From the image it is obvious that the indium atoms have been incorporated in the surface through steps: the terraces are not populated uniformly by indium, the impurities are found only in the direct vicinity of the steps. This behavior is identical to what has been observed for indium adatoms on a Cu(1117) surface [25]. Once

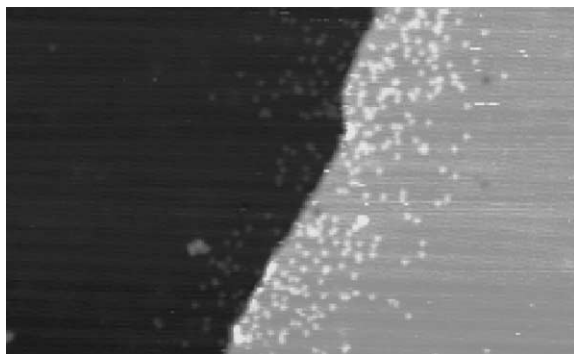


Fig. 1.  $662 \times 404 \text{ \AA}^2$  STM image of a monatomic height step on a Cu(001) surface taken 38 min after the deposition of 0.03 ML of indium at room temperature. Embedded indium atoms show up as bright dots with a height of  $0.4 \text{ \AA}$ . The image shows a high density of embedded indium atoms near the step ( $V_t = -1.16 \text{ V}$ ,  $I_t = 0.1 \text{ nA}$ ).

the indium adatoms have reached a step and attached themselves to it, they invade the first layer on both sides of the step and over time slowly infiltrate the entire first layer of the crystal. At room temperature it takes the indium atoms typically several hours to spread homogeneously through the entire surface.

The spreading of the indium atoms through the first layer implies that they are somehow able to diffuse, whilst remaining embedded within the surface. The diffusion behavior of the embedded indium atoms was studied by making series of images of the same area on the copper surface to form an STM movie of the motion [26].

The diffusion behavior of the indium atoms in these images is unusual in several respects, as is illustrated by the STM images in Fig. 2.

- The jumps of the indium atoms are separated by very long time intervals. At room temperature these intervals can be as long as a few minutes.
- If the indium atoms move between two images, they typically move over several atomic spacings. Naïvely one would expect them to make single, monatomic hops.
- Nearby indium atoms show a strong tendency to make their jumps simultaneously. If the indium atoms move independently from one another, they should not exhibit such concerted motion.

To explain the unusual diffusion behavior we invoke the existence of an assisting particle. First of all, as the assisting particle is invisible in the STM-images we have to assume that it is too mobile to be imaged with the STM. Second, if the assisting particle is present in very low numbers only, this could account for the long waiting times. Third, a multiple encounter between the assisting particle and the indium atoms may lead to a jump over several atomic spacings. And finally, if the assisting particle helps to displace one indium atom, there is a high probability that nearby indium atoms will also be displaced, leading to a concerted motion of the indium atoms. It will be shown in Section 4 that also the shape of the distribution of jump lengths forms direct evidence for a mechanism in which the motion is only possible by virtue of an assisting entity.

We now consider the following possibilities:

- Diffusion of embedded atoms with assistance of an adsorbed residual gas molecule.
- Diffusion of embedded atoms through exchange with copper adatoms.
- Diffusion of embedded atoms through exchange with surface vacancies.

If the diffusion of an embedded indium atom were assisted by an adsorbed molecule from the residual gas in the vacuum system, the rate of long jumps of the indium atoms should depend on the rate at which these gas molecules are adsorbed. The diffusion mechanism could be similar to the one that was observed for Pt on Pt(110) [27], where enhanced diffusion of a Pt adatom was enabled by adsorption of a H atom. For the diffusion of the indium atoms, such a mechanism can however not be active. After desorption of the residual gas molecule, it is no longer present on the surface and is therefore not available to assist other indium atoms in making long jumps. The simultaneous jumps of the indium atoms cannot be explained with this mechanism. Secondly, as we will see in Section 4, the rate of long jumps depends strongly on the surface temperature. For the adsorption rate from the residual gas in a UHV system, such a dependence should not be expected. Third, the length of the long jumps will depend on

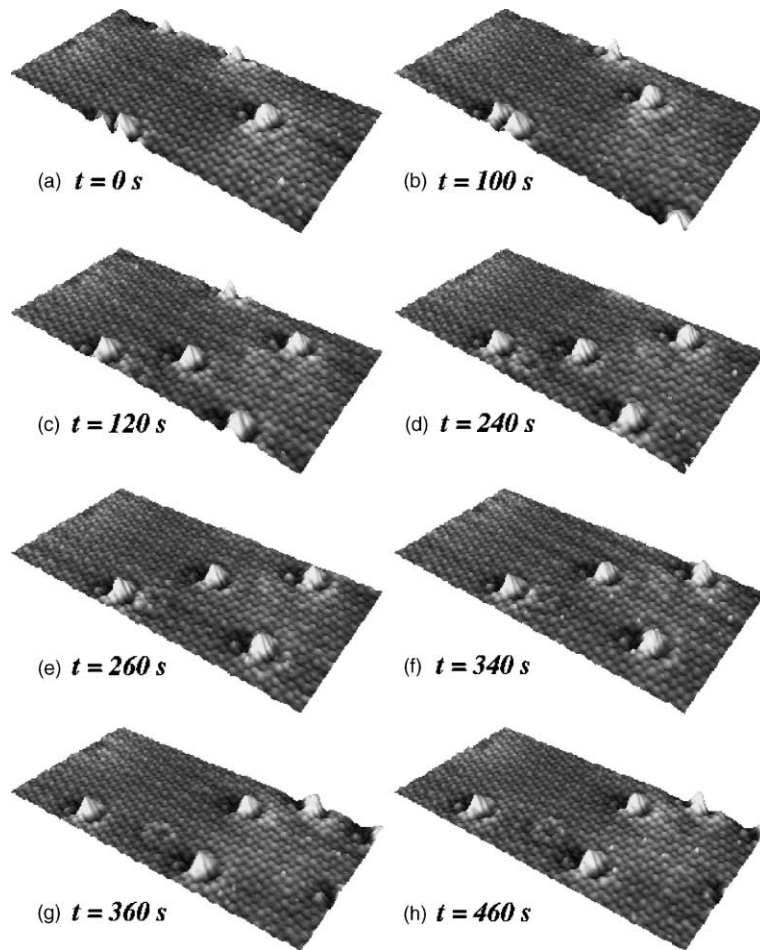


Fig. 2.  $140 \times 70 \text{ \AA}^2$  STM images of the Cu(001) surface at room temperature illustrating the diffusion of embedded indium atoms. (a) shows five embedded indium atoms. The right hand panel (b) shows that after 100 s the indium atoms still occupy the same lattice sites. (c) shows the next image in which all indium atoms have made a multi-lattice-spacing jump. After this jump the indium atoms again stay at the same lattice site for another 2 min, illustrated by (d). (e–h) show that this pattern of long jumps separated by long time intervals repeats itself ( $V_t = -0.58 \text{ V}$ ,  $I_t = 0.9 \text{ nA}$ ).

how long the residual gas molecule resides at the indium atom. As the residence time of the molecule goes down exponentially with temperature, the jump length of the indium atom should do the same. This is definitely not what we observe (Section 4). Diffusion of the indium atoms with the assistance of adsorbed gas molecules can thus be ruled out.

This leaves the possibility of place exchange with either a copper adatom or a surface vacancy. For exchange with a copper adatom the diffusion mechanism is illustrated in Fig. 3. In the mea-

surements, embedded indium atoms are observed to make jumps of several atomic spacings. For the adatom mechanism, this would imply that the indium adatoms reinsert themselves into the terrace after making at most a few hops. However, as was already seen in low temperature measurements [25], after deposition on the Cu(001) surface, indium adatoms do not insert themselves into the first layer. Instead they perform a random walk on top of the Cu(001) surface and attach to steps. The same conclusion can be drawn from the room temperature deposition experiment, in which the

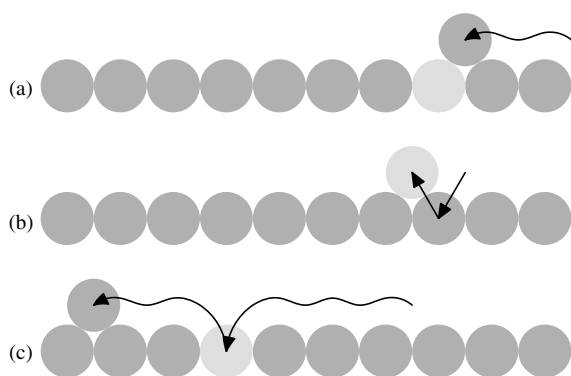


Fig. 3. A cross-sectional view of an exchange process of indium (bright) with a copper (dark) adatom, leading to a long jump of the indium atom. (a) A copper adatom arrives at the embedded indium site, either through normal hopping or exchange hopping (not shown). (b) The copper adatom changes places with the indium atom. (c) The indium adatom now makes one or more hops over the surface before it reinserts itself into the first layer. A multiple encounter between the copper adatom and the indium may lead to even larger displacements.

indium is deposited homogeneously onto the surface. The adatom mechanism would lead to a homogeneous distribution of embedded indium atoms directly after deposition. By contrast, Fig. 1 clearly shows a high density of embedded indium atoms near a step shortly after deposition. The copper adatom exchange mechanism can therefore be ruled out with confidence. We identify the exchange with surface vacancies as the mechanism responsible for the observed diffusion of indium through the surface. Fig. 4 illustrates the vacancy-mediated diffusion mechanism.

Having shown that the diffusion of indium in Cu(001) is vacancy-mediated, we now argue why the vacancies never show up in the STM images, by use of energies from embedded atom calculations.<sup>2</sup> Using the formation energy of a surface vacancy in Cu(001) of 517 meV, we predict a density of vacancies of  $1 \times 10^{-9}$  at room temper-

<sup>2</sup> EAM energies were calculated using the computer code of M. Breeman, Rijksuniversiteit Groningen. The absolute value of the diffusion barriers was divided by 1.7 to accommodate the consistent overestimation of the diffusion barriers in these calculations.

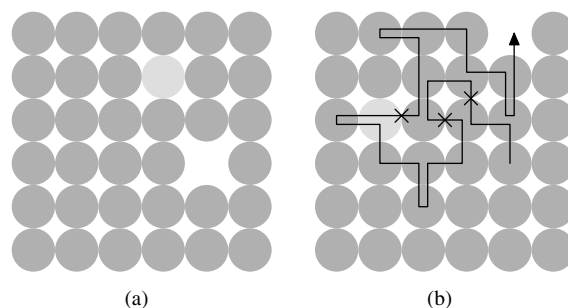


Fig. 4. A ball-model (top view) of a diffusion event in which the passage of a surface vacancy leads to a multi-lattice-spacing displacement of the indium atom (bright). The arrow indicates the random walk pathway of the vacancy, and the indium–vacancy exchanges are marked with crosses to show the pathway of the indium between its beginning and endpoints.

ature. Assuming an attempt frequency of  $10^{12}$  Hz, combined with the calculated diffusion barrier of 0.35 eV [15], we expect a vacancy jump rate of  $10^6$  Hz at room temperature. This means that we cannot “see” the vacancies for two reasons. At every instant in time the probability for even a single vacancy to be present in the STM scan area is very low. The rate at which each vacancy moves is much higher than the imaging rate of the STM and it also exceeds the bandwidth of the STM’s current preamplifier by several orders of magnitude. Lowering the temperature to slow the vacancies down would reduce the vacancy density even further, while increasing the temperature to create more vacancies would lead to an even higher vacancy mobility. It is therefore only via the artificial introduction of vacancies above the equilibrium concentration or through the vacancy-induced diffusion of tracer particles, such as the embedded indium atoms, that we can detect the presence and motion of the vacancies.

#### 4. Quantitative analysis

The vacancy-mediated diffusion mechanism of indium atoms in a Cu(001) surface provides an unprecedented opportunity to probe the properties of monatomic surface vacancies. The role of the indium atom is that of the tracer particle. Since it can be detected with the STM it reveals precisely

when a vacancy passed through the imaged region, and its displacement provides a measure for how many encounters the indium atom has had with the vacancy. In this section a quantitative analysis of the diffusion of embedded indium atoms is presented and is used to evaluate some of the fundamental energy parameters of surface vacancies.

#### 4.1. Jump length distribution

The diffusion of indium atoms in the surface proceeds through multi-lattice-spacing jumps separated by long time intervals. The multi-lattice-spacing nature of the diffusion is illustrated by the jump vector distribution which is plotted in Fig. 5. The jump vector distribution shows that there is a significant probability for the indium atom to jump as far as five or six atomic spacings. In terms of the vacancy-mediated diffusion mechanism, if the vacancy were making an ordinary random walk and were not influenced by the presence of the indium, standard random walk theory [28]

gives that on average the vacancy and the indium atom must change places as often as 20 to 30 times to give such a large displacement.

In paper II and in Ref. [14] we have derived that for the vacancy-mediated diffusion mechanism, one expects the shape of the length distribution of the long jumps to be that of a modified Bessel function of order zero. To verify this, the data of Fig. 5 were replotted in Fig. 6 as the radial jump length distribution function. Fig. 6 contains six plots for the distribution at different temperatures. Each distribution can be fitted very well with the modified Bessel function, confirming the vacancy-mediated diffusion mechanism for the indium atoms. Discrepancies between the expected and measured probabilities for jumps of unit length are an artifact of the automated procedure that was used to analyse the images [29].<sup>3</sup> For comparison, one of the panels contains the best-fit Gaussian curve that should be followed for ordinary, i.e. non-assisted diffusion. The only free parameter used in the fits is the recombination probability  $\hat{p}_{\text{rec}}$  for vacancies at steps, between subsequent encounters with the same indium atom [15]. This probability is directly related to the average terrace width (see the paper II and Section 4.4). The terrace widths that are extracted from the fitting procedure are all within a factor 2.5 of the “average” terrace width of 400 atomic spacings that was used in the model calculations of paper II. The variations in this number can be ascribed to the proximity of steps. The effect of steps will be discussed in more detail in Section 4.4.

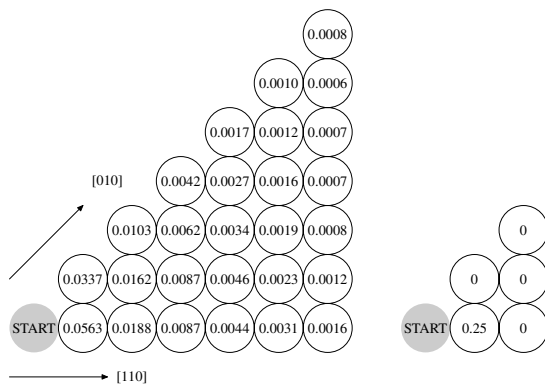


Fig. 5. The distribution of jump vectors measured from 1461 jumps that were observed in STM movies at 319.5 K. Plotted is the probability for jumps of an indium atom from its starting position to each of the non-equivalent lattice sites shown. Probabilities have been normalized so that the probabilities for the entire lattice (not just the non-equivalent sites) add up to one. In contrast to the calculations in paper II [15], the probability for a jump of length zero cannot be measured with the STM and has been put to zero. To illustrate the unusual diffusion behavior, the jump vector distribution for the case of simple hopping is plotted to the right.

#### 4.2. Waiting time distribution

One of the unusual aspects of the diffusion of embedded indium atoms is the long waiting time between consecutive jumps. The distribution of waiting times, expressed here in number of images, has been plotted for six different temperatures in Fig. 7. As can be seen from the figure, all measured

<sup>3</sup> Noise in the STM images will sometimes cause the detected center of mass of an indium atom to shift by more than one atomic spacing, thereby triggering a monatomic length jump at too short a time interval.

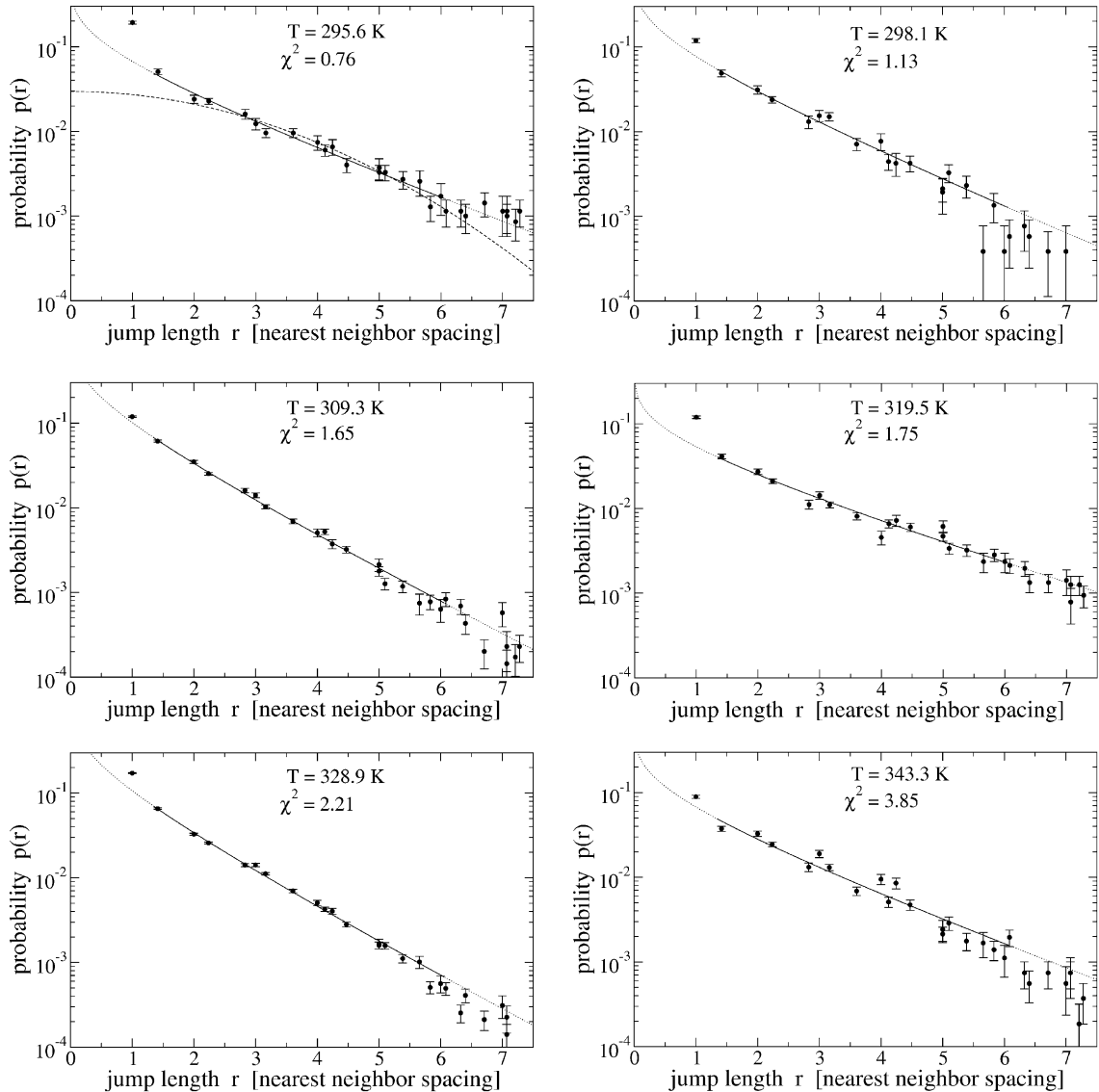


Fig. 6. Radial jump length distribution for embedded indium atoms measured for six different temperatures. The data points have been fitted with the modified Bessel function of order zero that is expected for the vacancy-mediated diffusion mechanism [14,15]. The fits were made to the data points for jump lengths from  $\sqrt{2}$  to 6, as indicated by the solid part of the curve in each panel. The normalized goodness of fit  $\chi^2$  for this range is indicated. The dashed curve in the upper left panel is the best-fit Gaussian curve for the same data range.

distributions are purely exponential, with a time constant  $\tau$  that decreases with increasing temperature. The exponential shape of the distributions shows that the waiting time of an indium atom to its next long jump is governed by a Poisson process

with rate  $\tau^{-1}$ . This implies that subsequent long jumps are independent, which we take as proof that they are caused by different vacancies. The vacancies are created independently at random time intervals. The frequency with which a specific

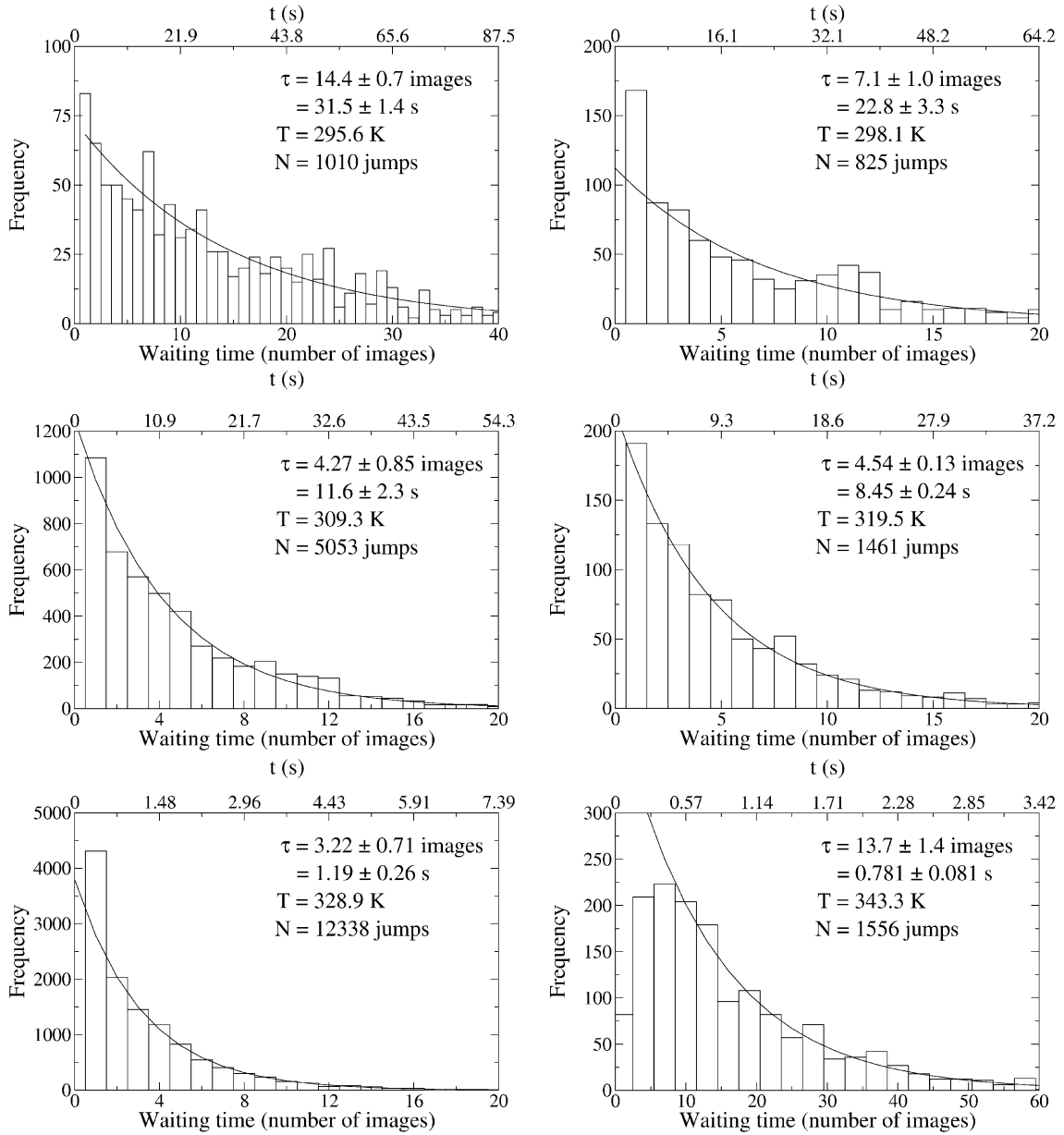


Fig. 7. Waiting time distributions measured for six different temperatures. All fits are pure exponentials. The time constant  $\tau$  is shown in the graph for each of the distributions. Too high or too low count rates at short waiting times are an artifact of the automated analysis scheme of the images [29] (refer footnote 3) and are ignored in the fits.

lattice site of the Cu(001) surface is visited by new vacancies is  $\tau^{-1}$ . This frequency is such that our STM can easily keep up with the diffusion process up to a temperature of 350 K.

#### 4.3. Temperature dependence of the jump frequency

Simple surface diffusion processes are governed by a single diffusion barrier  $E_D$ , which the diffusing



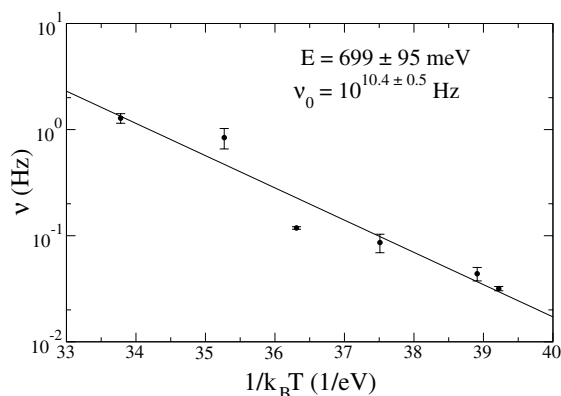


Fig. 8. Arrhenius plot of the rate of long jumps of the embedded indium atoms. The activation energy and attempt frequency are shown in the graph (see also Fig. 11).

species has to overcome to hop from one potential well to the next. To verify whether the diffusion of embedded indium atoms in a Cu(001) surface is indeed a thermally activated process, the average jump rate of the embedded indium atoms has been plotted as a function of  $1/k_B T$  in Fig. 8. The figure shows that the diffusion of embedded indium atoms through the Cu(001) surface is indeed a thermally activated process with an activation energy of 699 meV and an attempt frequency of  $10^{10.4}$  Hz. As will be discussed in Section 6, Fig. 8 does not imply that the process is governed by a single activation energy.

#### 4.4. Mean square displacement

The mean square jump length of the indium atoms is a direct measure for the number of encounters that an indium atom has on average with a single passing vacancy. From the six jump length distributions that were shown in Section 4.1, the mean square jump length has been measured. The results are shown in Table 1. The values in Table 1 exhibit a seemingly random variation that is much larger than the statistical error margins. As discussed in paper II [15], we should expect  $d^2$  to depend only logarithmically on the terrace width. Given the fact that all measurements were performed on terraces with a typical width of a few hundred Angstroms, the considerable variation in

Table 1

Measured mean square displacement as a function of temperature

$T$ (K)	$\langle u^2 \rangle (\text{latt.spac.}^2)$
295.6	$4.37 \pm 0.11$
298.1	$4.16 \pm 0.13$
309.3	$3.61 \pm 0.04$
319.5	$7.67 \pm 0.15$
328.9	$2.82 \pm 0.02$
343.3	$5.15 \pm 0.12$

the mean square jump length with temperature is unexpected.

It is at this point that the precise details of the measurements become important. After the deposition of the indium the room temperature measurements were performed and the temperature was then raised to the values shown in Table 1. Each time after raising the temperature, the STM was allowed to stabilize its temperature to the point where the STM images showed no lateral thermal drift. A suitable area on a terrace was then selected to perform the diffusion measurements at that specific temperature. No effort was undertaken to select the same area at all six temperatures. As an example the region that was selected for the 343.3 K measurements is shown in Fig. 9. From each of the overview scans that were made prior to starting the diffusion measurements, the distance to the steps surrounding the measurement site was quantified by measuring both the loga-



Fig. 9.  $2495 \times 1248 \text{ \AA}^2$  STM image of the Cu(001) surface at 343.3 K. The surface area that was selected to perform the diffusion measurements at this temperature is indicated by the rectangle. The trajectory to the nearest step has been drawn in the figure. The length of this trajectory is shown in Table 2 ( $V_t = -1.16 \text{ V}$ ,  $I_t = 0.1 \text{ nA}$ ).

Table 2  
Measured nearest-step-distances as a function of temperature

$T$ (K)	$\ln(d_{\text{step,min}})$	$\langle \ln(d_{\text{step}}) \rangle$	$\langle u^2 \rangle$
295.6	4.52	4.90	4.37
298.1	4.46	4.61	4.16
309.3	4.32	4.45	3.61
319.5	5.10	5.44	7.67
328.9	4.48*	4.56*	2.82
343.3	4.93	5.22	5.15

All distances have been measured in Cu(001) atomic spacings. The two values marked with a \* are estimated values: the overview scan at 328.9 K showed only a part of the relevant surroundings of the area that was used to obtain the jump data.

rithm of the minimum distance to a step as well as the polar average of the logarithm of the distance to the steps. The measured values are shown in Table 2.

Both ways to quantify the proximity of steps to the measurement site show that there is a very clear trend for longer jumps when the steps are further away. This trend is even more clear from Fig. 10, where the mean square jump length is plotted versus the average logarithm of the distance of the measurement site to a step. In this graph the 328.9 K measurement has not been used as the measurement area was partly outside the area that was imaged in the overview scan and the

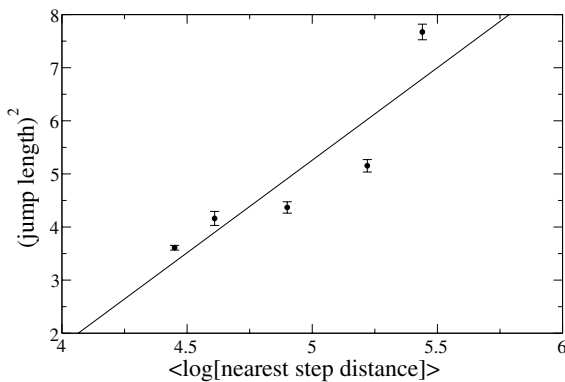


Fig. 10. Plot of the mean square jump length versus the average logarithm of the distance of the measurement area to the steps. The graph shows that measurements that are made further away from a step yield larger jump lengths. All distances were measured in atomic spacings.

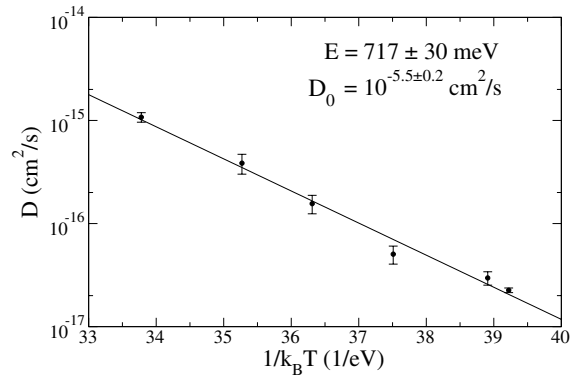


Fig. 11. Arrhenius plot of the diffusion coefficient  $D$  of embedded indium atoms. The coefficient  $D$  was calculated at each temperature by multiplying the rate of long jumps (Fig. 8) with the mean-square jump length (Table 1).

distance to the surrounding steps could not be properly determined.

Because all measurements were performed in thermodynamic equilibrium, the density of vacancies throughout the terraces is constant. The observation that the jump length of the indium atoms depends on the specific geometry in which the measurements were performed therefore implies that the rate of long jumps is also position dependent. This in turn means that since all measurements were performed at different areas, the temperature dependence of the diffusion of embedded indium atoms can only be properly measured by plotting the diffusion coefficient  $D$  of the indium atoms versus  $1/k_B T$  as opposed to the jump rate versus  $1/k_B T$  which was plotted in Fig. 8. This has been done in Fig. 11. We observe that the scatter that was present in Fig. 8 is significantly reduced and a much more accurate value of  $717 \pm 30$  meV for the activation energy is obtained.

## 5. A vacancy attachment barrier?

Indium atoms that are incorporated into the first layer of the Cu(001) surface at room temperature via a step appear to have a slight preference for the upper terrace with respect to the lower terrace. This effect can be seen from Fig. 1 where  $\approx 60\%$  of the indium atoms have entered the upper

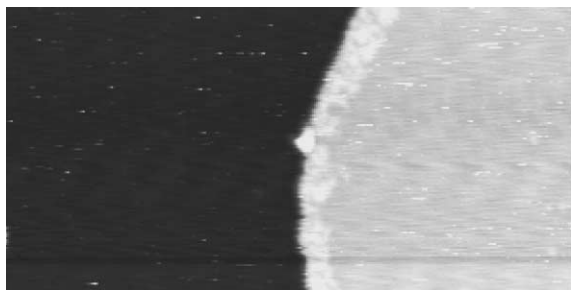


Fig. 12.  $830 \times 415 \text{ \AA}^2$  STM image of indium being incorporated into the upper terrace on the right hand side of a step on the Cu(001) surface. The image was taken at a temperature of 280.4 K during a slow ramp of the temperature from 130 K, the temperature where 0.015 ML of indium was deposited on clean Cu(001). The indium first started to be incorporated into the upper terrace at 267 K and shows up as a light band on the right hand side of the step ( $V_t = -0.67 \text{ V}$ ,  $I_t = 0.1 \text{ nA}$ ).

terrace and only 40% have gone into the lower terrace. The effect is even more dramatic if the incorporation of the indium takes place at temperatures below room temperature. Fig. 12 shows an image that was obtained at 280.4 K, after indium had been deposited on the surface at 130 K and was first observed to be incorporated into the surface at a temperature of 270 K. The image shows that practically all the indium atoms enter the upper terrace at this temperature. This observation may imply the existence of a step edge barrier, similar to the Schwoebel barrier for adatoms [30–32], but in this case for the attachment of surface vacancies at the lower side of a step. Using the ratio of the number of indium atoms that is incorporated into the upper and lower terraces at 270 K (only between 1% and 2% of the indium atoms is incorporated into the lower terrace) and 300 K, we derive a first estimate of this barrier of 0.8 eV. The difference in incorporation between the upper and lower terrace has already been discussed in the context of the Mn/Cu(001) surface alloy [23,33,34] and can in principle be attributed to the difference in the incorporation processes for the upper and lower terrace. However, the high value of 0.8 eV suggests that other factors play a role in the preferred incorporation into the upper terrace. One such factor could be the large amount of indium that is present at the step during incorporation.

## 6. Interpretation of the activation energy

By definition, the rate at which the indium atom is displaced by a surface vacancy is the product of the vacancy density at the site next to the indium atom times the rate at which vacancies exchange with the indium atom. The activation energy obtained from the temperature dependence of the total displacement rate will yield the sum of the vacancy formation energy and the vacancy diffusion barrier. When the measurements are performed with a finite temporal resolution and if there is an interaction present between the vacancy and the indium atom, this simple picture changes.

The energy landscape for the vacancy is sketched in Fig. 13. We now consider the situation where the diffusion is observed with a finite time resolution. We assume that the time resolution of the STM-measurements is sufficient to resolve the effect of the entire random walk of one individual vacancy from that of the next, which was already shown to be the case in Section 4.2. The starting situation is shown in Fig. 14: an indium atom is embedded in the origin of a square lattice with a vacancy sitting next to it at (1,0). The only diffusion barrier that has been modified by the indium atom is the one which is associated with the

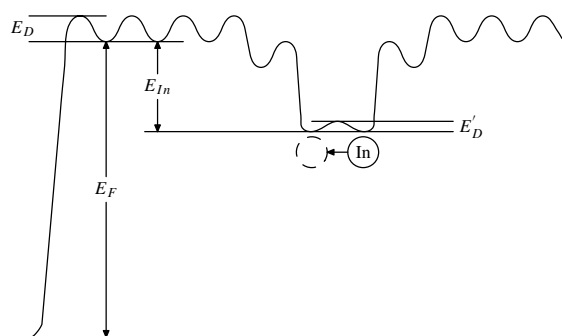


Fig. 13. One-dimensional energy landscape for a vacancy in the Cu(001) surface. For this one-dimensional situation the vacancy is formed at the step on the left and approaches the indium from there. It is only able to displace the indium atom to the left by one atomic spacing.  $E_F$  is the formation energy of a Cu(001)-vacancy,  $E_D$  is the diffusion barrier for a Cu(001)-vacancy,  $E'_D$  is the vacancy–indium exchange barrier and  $E_{In}$  is the binding energy for an indium–vacancy pair.

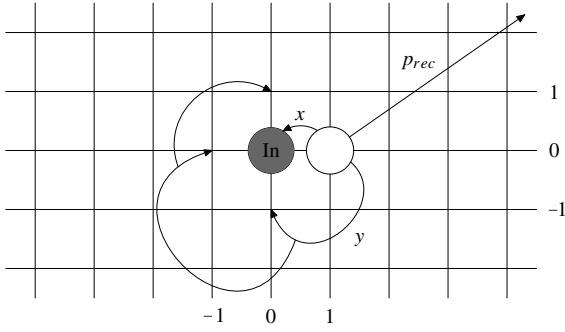


Fig. 14. The random walk starting situation, with the vacancy directly next to the indium atom. The probabilities  $x$ ,  $y$  and  $p_{rec}$  are introduced in the text.

vacancy–indium exchange. This is equivalent to putting  $E_{In} = 0$  in Fig. 13.

We now define the following additional quantities:

- $x$  The probability that in the first step the vacancy immediately changes places with the indium.
- $y$  The probability that the vacancy does not immediately change places with the indium but that it returns to any of the four sites neighbouring the indium.
- $p_{rec}$  The recombination probability of the vacancy, i.e. the probability that the vacancy recombines at a step without ever changing places with the indium. This probability is determined by the distances to the nearby steps.

Note that  $x + y + p_{rec} \neq 1$ , because, as is indicated in Fig. 14, there is the possibility that the vacancy returns one or more times to the sites neighbouring the indium atom and then recombines, without ever exchanging with the indium. Only if one were to define the recombination probability as  $p'_{rec}$ , the probability that the vacancy recombines without first returning to any of the sites neighbouring the indium atom, would  $x + y + p'_{rec} = 1$ . The rate at which jumps of the indium are registered by the STM is determined by the rate at which total displacements with a length of at least one atomic spacing occur. Given the starting sit-

uation of Fig. 14, the probability that the indium is displaced by the vacancy is given by

$$p_{dis} = 1 - p_{rec} = x + y \cdot (x + y \cdot (x + y \cdot (\dots)))$$

$$= \sum_{N=0}^{\infty} y^N \cdot x = \frac{x}{1 - y} \quad (1)$$

The In atom is displaced if the vacancy returns to any of the four sites neighboring the In atom 0, 1, 2, etc. times, then exchanges place with it. The possibility that multiple displacements of the indium may add up to a zero net displacement is ignored.<sup>4</sup> The precise value of  $x$ , the probability to make a successful exchange, is determined by the energy difference between the modified and unmodified vacancy exchange barrier,  $E_D - E'_D$ .

$$x = x(T) = \frac{v_0 e^{-\frac{E'_D}{k_B T}}}{v_0 e^{-\frac{E'_D}{k_B T}} + 3v_0 e^{-\frac{E_D}{k_B T}}} = \frac{1}{1 + 3e^{-\frac{E_D - E'_D}{k_B T}}} \quad (2)$$

Upon examining the random walk of the vacancy when it has not exchanged with the indium but has returned to any of the sites neighbouring the indium, we see that only the first step of this random walk pathway has a temperature dependent probability associated with it and  $y$  can therefore be split up in a temperature dependent and a temperature independent part

$$y = y(T) = (1 - x(T))C \quad (3)$$

where  $0 \leq C \leq 1$  is a constant which is determined by the geometry of the lattice, and especially by the distribution of distances between the starting position of the vacancy and the absorbing boundaries (steps). It can be evaluated numerically. Substituting Eq. (3) in Eq. (1), the probability to have at least one displacement is equal to

$$p_{dis} = \frac{x(T)}{1 - y(T)} = \frac{x(T)}{1 - (1 - x(T)) \cdot C}$$

$$= \frac{x(T)}{(1 - C) + Cx(T)} = \frac{1}{1 + 3(1 - C)e^{-\frac{E_D - E'_D}{k_B T}}} \quad (4)$$

<sup>4</sup> This is justified by numerical calculations presented in paper II where we address this problem for the case of indium. Our calculations show that the fraction of jumps that have a zero net length changes only marginally with temperature.

From Eq. (4) it is clear that the final rate of long jumps will contain exponential terms not only in the numerator, but also in the denominator. The rate of long jumps should not show normal thermally activated Arrhenius behavior. The observed rate of long jumps is equal to the equilibrium rate at which vacancies exchange with the indium atom, divided by the average number of elementary displacements caused by a single vacancy, given that the vacancy has displaced the indium atom at least once. This average number of displacements  $\langle n \rangle$  is given by

$$\begin{aligned} \langle n \rangle &= 1 + 0 \cdot p_{\text{rec}} + 1 \cdot (1 - p_{\text{rec}})p_{\text{rec}} \\ &\quad + 2 \cdot (1 - p_{\text{rec}})^2 p_{\text{rec}} + \dots \\ &= \frac{1}{p_{\text{rec}}} = \frac{1}{1 - C} \left( \frac{1}{1 - x(T)} - C \right) \\ &= 1 + \frac{e^{\frac{E_D - E'_D}{k_B T}}}{3(1 - C)} \end{aligned} \quad (5)$$

Using Eq. (5), the observed rate of long jumps is equal to

$$v_{\text{LJ}} = v_0 \frac{e^{-\frac{E_F + E_D + \Delta}{k_B T}}}{1 + \frac{e^{-\frac{\Delta}{k_B T}}}{C'}} \quad (6)$$

where

$$C' = 3(1 - C)$$

$$\Delta = E'_D - E_D$$

In the case that indium is “identical” to copper, so that  $\Delta = 0$ ,  $\langle n \rangle$  becomes  $(4 - 3C)/3(1 - C)$  and the rate of long jumps reduces to

$$v_{\text{LJ}} = v_0 \frac{e^{-\frac{E_F + E_D}{k_B T}}}{1 + \frac{1}{C'}} = \frac{v}{1 + \frac{1}{C'}} \quad (7)$$

where  $v$  is the jump rate of atoms in the clean Cu(001) surface. The denominator corresponds to the number of exchanges contributing to a long jump.

In the extremely repulsive case  $\Delta/(k_B T) \gg 1$  and the average number of displacements  $\langle n \rangle$  becomes approximately equal to 1. Eq. (6) reduces to

$$v_{\text{LJ}} = v_0 e^{-\frac{E_F + E_D + \Delta}{k_B T}} = v_0 e^{-\frac{E_F + E'_D}{k_B T}} \quad (8)$$

In the extremely attractive case  $\Delta/(k_B T) \ll -1$  and the average number of jumps  $\langle n \rangle$  is  $(1/(1 - C)) \cdot (1/3)e^{-\Delta/(k_B T)}$ . Eq. (6) now reduces to

$$v_{\text{LJ}} = 3v_0(1 - C)e^{\frac{E_F + E_D}{k_B T}} \quad (9)$$

We immediately see the fundamental difference between attraction and repulsion. The apparent activation energy for strong attraction is identical to that for the copper surface itself, while it is larger in the case of repulsion. This asymmetry between attraction and repulsion is caused by the fact that for moderate to strong attraction, the probability  $x$  rapidly approaches unity, meaning that the arrival of a vacancy next to the indium is almost guaranteed to cause a long jump. In contrast, in the case of repulsion, the probability  $x$  scales with the Boltzmann-factor containing the exchange barrier of the vacancy and the embedded atom.

In general, the Arrhenius plot of the log of the rate of long jumps versus  $1/(k_B T)$  is non-linear:

$$\begin{aligned} \ln(v_{\text{LJ}}) &= \ln(v_0) - (E_F + E_D + \Delta) \frac{1}{k_B T} \\ &\quad - \ln \left( 1 + \frac{e^{-\frac{\Delta}{k_B T}}}{C'} \right) \end{aligned} \quad (10)$$

The last term on the right describes the departure from ideal Arrhenius behavior. With this term expanded to second order in  $1/(k_B T)$ , the rate of long jumps can be rewritten as

$$\begin{aligned} \ln(v_{\text{LJ}}) &= \ln \left( v_0 \frac{C'}{1 + C'} \right) + \left( -E_F - E_D \right. \\ &\quad \left. + \left( \frac{1}{1 + C'} - 1 \right) \Delta \right) \frac{1}{k_B T} \\ &\quad - \frac{C' \Delta^2}{2(1 + C')^2} \frac{1}{(k_B T)^2} + \dots \end{aligned} \quad (11)$$

For practical values of  $1/(k_B T)$  we are in the limit  $\Delta/(k_B T) \ll -1$  and the measured activation energy is equal to the sum of the vacancy formation energy,  $E_F$ , and the vacancy diffusion barrier,  $E_D$ .

We mention again that the fact that multiple displacements of the indium may actually add up to zero is ignored. The numerical calculations in paper II [15] show that for indium  $\approx 8.5\%$  of all long jumps have a net displacement of zero atomic

spacings. This fraction varies over the investigated temperature range by an insignificant amount and will therefore only result in a small modification of the prefactor in the temperature dependence.

## 7. Discussion

The jump length distributions mentioned in this work all have the shape that is expected for the particle-assisted diffusion mechanism. All distributions can be accurately fitted with the modified Bessel function, reconfirming that the diffusion of indium through the first layer takes place with the aid of some particle, which we deduced to be a vacancy by looking in detail at the incorporation process of the indium atoms. Having used the jump length distributions to validate the model described in the accompanying paper, we can now use this model to calculate the diffusion coefficient of copper atoms in a clean Cu(001) surface. This involves no more than taking the interaction between the vacancy and the indium atom out of the model such that the vacancy performs an unbiased random walk. At room temperature the average jump length of copper atoms in the clean Cu(001) surface is calculated to be 1.6 atomic spacings. Using the rate of long jumps of the indium atoms that was measured at room temperature we find that the diffusion coefficient of surface atoms in the Cu(001) surface as a result of vacancy mediated diffusion is  $0.42 \text{ \AA}^2 \text{ s}^{-1}$ . Using the attempt frequency that was obtained from Fig. 8, we find that at room temperature every site on the surface is visited by a new vacancy on average once every 32 s.

The sum of the Cu(001) surface vacancy formation and migration energy is equal to  $717 \pm 30$  meV. The sum of the EAM calculated diffusion barrier (0.35 eV) and the formation energy (0.52 eV) amounts to 0.86 eV. The fact that this result is too large is not entirely unexpected as all diffusion barriers that were calculated with EAM were too large when compared with experiments. However, the value of 0.35 eV was already obtained by dividing the true EAM value by a factor 1.7 (refer footnote 2). Using the measured sum and the calculated EAM formation energy of 0.52 eV, we find a lower value of 0.20 eV for the diffusion

barrier of a Cu(001) surface vacancy. Using the vacancy formation energy of 0.485 eV from [24] that was obtained through first-principles calculations we obtain a vacancy diffusion barrier of 0.232 eV. With such a low diffusion barrier, we expect a room temperature vacancy diffusion rate of  $10^8$  Hz.

The interpretation of the activation energy as the sum of the vacancy diffusion barrier and the vacancy formation energy is supported by measurements of vacancy-mediated diffusion of Pd in Cu(001) [24], which reveal a value of  $0.88 \pm 0.03$  eV for the sum of the vacancy formation energy and the Pd-vacancy exchange barrier. The higher activation energy is a direct consequence of the fact that vacancies and embedded palladium atoms repel (see Section 6). To be able to experimentally separate out the two energy parameters, the vacancy formation energy and the vacancy diffusion barrier, independent measurements are needed of one of the two energies. One possibility is to follow artificially created surface vacancies at low temperature [35–37]. Such a measurement would yield the diffusion barrier for a monatomic surface vacancy which could then be combined with the 717 meV that we measured to obtain the vacancy formation energy.

The variation in mean square jump length that was observed with the distance to the nearest step confirms the idea that surface vacancies are formed and annihilated at steps. The creation of a surface vacancy through the expulsion of an atom from a section of flat Cu(001) terrace has been predicted to cost 984 meV [38]. Because of this high energy for the creation of an adatom-vacancy pair, at most temperatures surface vacancies are formed almost exclusively at steps. This means that the steps section the surface into separated areas through which the vacancies are allowed to diffuse. The vacancies are annihilated when they reach a step. A vacancy which exchanges with an indium atom near a step has a relatively high probability to recombine at the step as opposed to making another exchange with the indium atom. Indium atoms near a step will therefore on average make shorter jumps than indium atoms that are far away from a step. Given a constant density of surface vacancies throughout the terrace (the

measurements were performed in thermal equilibrium), this implies that the rate of long jumps near steps will be higher than in the middle of a terrace. Hence, the indium will perform relatively many jumps of a short length near a step, whereas in the middle of a wide terrace, indium atoms will tend to jump less frequently, but given the increased lifetime of the vacancy, they will jump over longer distances. This observation opens the way to detailed studies of vacancy creation and annihilation near steps and kinks.

The existence of the vacancy attachment barrier that was suggested in Section 5 needs to be investigated in more detail. The influence of the considerable amount of indium that was present at the step makes it hard to draw detailed conclusions about this barrier. Step fluctuations may provide a low energy pathway for the indium atoms to be incorporated in the upper terrace. Further experiments investigating the existence and magnitude of this barrier at a clean step should be performed with low densities of embedded guest atoms, e.g. in adatom or vacancy islands. The lifetime of a surface vacancy in such islands will be affected strongly by the presence of this barrier. If present, the barrier will lead to significant differences in the mean square jump length and frequency of long jumps of indium atoms embedded in equal-size adatom and vacancy islands.

## 8. Conclusions

Surface vacancies were shown to be responsible for the motion of embedded indium atoms in the Cu(001) surface. The density of surface vacancies at room temperature is extremely low, but vacancies are able to diffuse through the surface at an extremely high rate. In the STM-measurements the rapid diffusion of these vacancies leads to simultaneous long jumps of embedded indium atoms. Measurements of the jump length and jump rate were performed at six different temperatures. These measurements show that the vacancy-mediated diffusion process can be accurately described with the model that is presented in paper II [15] and Ref. [14], provided that the interaction between the embedded indium and the

surface vacancies is properly taken into account. The role of steps as sources and sinks for surface vacancies has been confirmed by measuring the position dependent jump rate and jump length of the indium atoms. Near a step the jump rate of the indium atoms is increased, but at the same time, given the shorter lifetime of vacancies near a step, the jump length is decreased. The sum of the vacancy formation and migration energy was measured to be  $717 \pm 30$  meV.

The most far-reaching conclusion concerns the mobility of the Cu(001) surface itself. The diffusing vacancy leaves behind a trail of displaced surface copper atoms and thereby induces a significant mobility within the first layer of the surface, already at room temperature [13]. The mobility of atoms in the clean Cu(001) surface was evaluated by applying the model of Ref. [14] and paper II [15] with the interaction between the tracer particle and the vacancy ignored. Through this procedure the diffusion coefficient of Cu(001) surface atoms was measured to be  $0.42 \text{ \AA}^2 \text{ s}^{-1}$  at room temperature.

## Acknowledgements

We gratefully acknowledge B. Poelsema for help with the preparation of the Cu-crystal. We acknowledge L. Niesen and M. Roşu for valuable discussions. This work is part of the research program of the “Stichting voor Fundamenteel Onderzoek der Materie (FOM)”, which is financially supported by the “Nederlandse Organisatie voor Wetenschappelijk Onderzoek (NWO)”.

## References

- [1] G. Binnig, H. Rohrer, Ch. Gerber, E. Weibel, Surface studies by scanning tunneling microscopy, *Phys. Rev. Lett.* 49 (1982) 57.
- [2] H.-C. Jeong, E.D. Williams, Steps on surfaces: experiments and theory, *Surf. Sci. Rep.* 34 (1999) 171.
- [3] Z. Zhang, M.G. Lagally, Atomistic processes in the early stages of thin-film growth, *Science* 276 (1997) 377.
- [4] L. Kuipers, M.S. Hoogeman, J.W.M. Frenken, Step dynamics on Au(110) studied with a high-temperature, high-speed scanning tunneling microscope, *Phys. Rev. Lett.* 71 (1993) 3517.

- [5] M. Poensgen, J.F. Wolf, J. Frohn, M. Giesen, H. Ibach, Step dynamics on Ag(111) and Cu(100) surfaces, *Surf. Sci.* 274 (1992) 430.
- [6] K. Morgenstern, G. Rosenfeld, B. Poelsema, G. Comsa, Brownian motion of vacancy islands on Ag(111), *Phys. Rev. Lett.* 74 (1995) 2058.
- [7] K. Morgenstern, E. Laegsgaard, F. Besenbacher, Brownian motion of 2D vacancy islands by adatom terrace diffusion, *Phys. Rev. Lett.* 86 (2001) 5739.
- [8] F. Besenbacher, Scanning tunneling microscopy studies of metal surfaces, *Rep. Prog. Phys.* 59 (1996) 1737.
- [9] H. Brune, Microscopic view of epitaxial metal growth: nucleation and aggregation, *Surf. Sci. Rep.* 31 (1998) 125.
- [10] G.L. Kellogg, Field ion microscope studies of single-atom surface diffusion and cluster nucleation on metal surfaces, *Surf. Sci. Rep.* 21 (1994) 1.
- [11] T.T. Tsong, Direct observation of interactions between individual atoms on tungsten surfaces, *Phys. Rev. B* 6 (1972) 417.
- [12] T.T. Tsong, *Atom-Probe Field Ion Microscopy*, Cambridge University Press, Cambridge, 1990.
- [13] R. van Gastel, E. Somfai, W. van Saarloos, J.W.M. Frenken, A giant atomic slide puzzle, *Nature (London)* 408 (2000) 665.
- [14] R. van Gastel, E. Somfai, S.B. van Albada, W. van Saarloos, J.W.M. Frenken, Nothing moves a surface: vacancy-mediated surface diffusion, *Phys. Rev. Lett.* 86 (2001) 1562.
- [15] E. Somfai, R. van Gastel, S.B. van Albada, W. van Saarloos, J.W.M. Frenken, Vacancy diffusion in the Cu(001) surface II: Random walk theory, *Surf. Sci.* 521 (2002) 26.
- [16] R.J.I.M. Koper, Surface Preparation Laboratory. Available from <<http://www.surface-prep-lab.com>>.
- [17] M.S. Hoogeman et al., Design and performance of a programmable-temperature scanning tunneling microscope, *Rev. Sci. Instr.* 69 (1998) 2072.
- [18] T. Klas, R. Fink, G. Krausch, R. Platzer, J. Voigt, R. Wesche, G. Schatz, Microscopic observation of step and terrace diffusion of indium atoms on Cu(111) surfaces, *Europhys. Lett.* 7 (1988) 151.
- [19] R. Fink, R. Wesche, T. Klas, G. Krausch, R. Platzer, J. Voigt, U. Wöhrmann, G. Schatz, Step-correlated diffusion of In atoms on Ag(100) and Ag(111) surfaces, *Surf. Sci.* 225 (1990) 331.
- [20] M.F. Roşu, F. Pleiter, L. Niesen, Interaction between Cu atoms and isolated  $^{111}\text{In}$  probe atoms on a Cu(100) surface, *Phys. Rev. B* 63 (2001) 165425.
- [21] J.B. Hannon, C. Klünker, M. Giesen, H. Ibach, N.C. Bartelt, J.C. Hamilton, Surface self-diffusion by vacancy motion: island ripening on Cu(001), *Phys. Rev. Lett.* 79 (1997) 2506.
- [22] T. Flores, S. Junghans, M. Wuttig, Atomic mechanisms for the diffusion of Mn atoms incorporated in the Cu(100) surface: an STM study, *Surf. Sci.* 371 (1997) 1.
- [23] T. Flores, S. Junghans, M. Wuttig, Atomic mechanism of the formation of an ordered surface alloy: an STM investigation of Mn/Cu(001), *Surf. Sci.* 371 (1997) 14.
- [24] M.L. Grant, B.S. Swartzentruber, N.C. Bartelt, J.B. Hannon, Diffusion kinetics in the Pd/Cu(001) surface alloy, *Phys. Rev. Lett.* 86 (2001) 4588.
- [25] R. van Gastel, M.F. Roşu, M.J. Rost, L. Niesen, J.W.M. Frenken, to be published.
- [26] The full movie is available at our website. Available from <<http://www-lion.leidenuniv.nl/groups/ip>>.
- [27] S. Horch, H.T. Lorensen, S. Helveg, E. Lægsgaard, I. Stensgaard, K.W. Jacobsen, J.K. Nørskov, F. Besenbacher, Enhancement of surface self-diffusion of platinum atoms by adsorbed hydrogen, *Nature (London)* 398 (1999) 134.
- [28] W. Feller, *An Introduction to Probability Theory and its Applications*, Wiley & Sons, New York, 1968.
- [29] M.J.J. Jak, C. Konstapel, A. van Kreuningen, J. Verhoveven, R. van Gastel, J.W.M. Frenken, Automated detection of particles, clusters and islands in scanning probe microscopy images, *Surf. Sci.* 494 (2001) 43.
- [30] R.L. Schwoebel, E.J. Shipsey, Step motion on crystal surfaces II, *J. Appl. Phys.* 37 (1966) 3682.
- [31] R.L. Schwoebel, Step motion on crystal surfaces II, *J. Appl. Phys.* 40 (1969) 614.
- [32] G. Ehrlich, F.G. Hudda, Atomic view of surface self-diffusion: tungsten on tungsten, *J. Chem. Phys.* 44 (1966) 1039.
- [33] G. Tréglia, B. Legrand, A. Saúl, T. Flores, M. Wuttig, Theoretical study of surface alloy formation through generation and annihilation of vacancies, *Surf. Sci.* 352 (1996) 552.
- [34] H. Ibach, M. Giesen, T. Flores, M. Wuttig, G. Tréglia, Vacancy generation at steps and the kinetics of surface alloy formation, *Surf. Sci.* 364 (1996) 453.
- [35] P. Molinàs-Mata, A.J. Mayne, G. Dujardin, Manipulation and dynamics at the atomic scale: a dual use of the scanning tunneling microscope, *Phys. Rev. Lett.* 80 (1998) 3101.
- [36] A.J. Mayne, F. Rose, C. Bolis, G. Dujardin, An scanning tunneling microscopy study of the diffusion of a single or a pair of atomic vacancies, *Surf. Sci.* 486 (2001) 226.
- [37] A. Kobayashi, F. Grey, E. Snyder, M. Aono, Probing local binding energy differences on the Si(001) $2 \times 1$  surface by field-induced atom extraction with the STM, *Surf. Sci.* 291 (1993) L739.
- [38] P. Stoltze, Simulation of surface defects, *J. Phys.: Cond. Matter* 6 (1994) 9495.